Science of the Total Environment 817 (2022) 152723

Contents lists available at ScienceDirect

Science of the Total Environment

journal homepage: www.elsevier.com/locate/scitotenv

Assessing the influence of urban greenness and green stormwater infrastructure on hydrology from satellite remote sensing

Gary Conley [a,*], Robert I. McDonald [b], Tyler Nodine [a], Teresa Chapman [c], Craig Holland [d], Christopher Hawkins [c], Nicole Beck [a]

[a] 2NDNATURE, 500 Seabright Avenue, Santa Cruz, CA 95062, USA
[b] Center for Sustainability Science, The Nature Conservancy, 10117 Berlin, Germany
[c] The Nature Conservancy in Colorado, 2424 Spruce Street. Boulder, CO 80302, USA
[d] The Nature Conservancy, 322 8th Avenue, New York, NY 10001, USA

HIGHLIGHTS

- Green stormwater infrastructure (GSI) is shown to affect urban greenness patterns.
- Urban greenness is shown to influence a range of downstream hydrologic responses.
- Only 9% of watersheds show significant trends in satellite-measured urban greenness.
- Detection of broad, watershed-scale GSI impacts is limited by GSI data completeness.

GRAPHICAL ABSTRACT

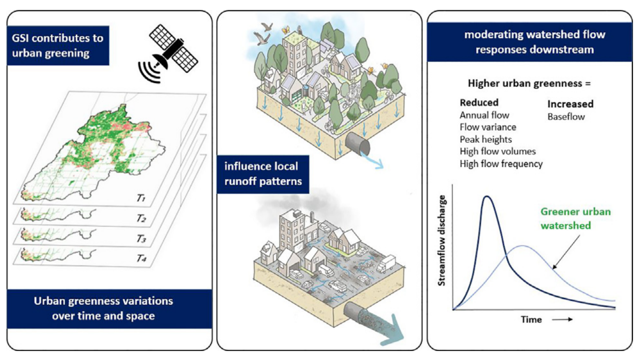

ARTICLE INFO

Article history:
Received 10 September 2021
Received in revised form 21 December 2021
Accepted 23 December 2021
Available online 31 December 2021

Editor: Ashantha Goonetilleke

Keywords:
Stormwater
Hydrology
Urban greenness
Green stormwater infrastructure
NDVI
Panel regression

ABSTRACT

Green stormwater infrastructure (GSI), which includes features like rain gardens, constructed wetlands, or urban tree canopy, is now widely recognized as a means to reduce urban runoff impacts and meet municipal water quality permit requirements. Many co-benefits of GSI are related to increased vegetative cover, which can be measured with satellite imagery via spectral indices such as the Normalized Difference Vegetation Index (NDVI). In urban landscapes, there remain critical gaps in understanding how urban greenness and GSI influence hydrology. Here, we quantify these relationships to assess the feasibility of tracking the effectiveness of urban greening for improving downstream hydrologic conditions. We combined hydrologic data from the United States Geological Survey (USGS) gauges with an NDVI time series (1985–2019) derived from Landsat satellite imagery, and synthesis of GSI implementation data from a set of 372 urbanized watersheds across the United States. We used a multivariate panel modeling approach to account for spatial and time varying factors (rainfall, temperature, urban cover expansion) in an effort to isolate the relationships of interest. After accounting for expansion of urban boundaries, only 32 watersheds (9%) showed significant greenness trends, a majority of which were reductions. Urban greenness had significant influences on downstream flow responses, so that on average, a 10% greenness increase showed a corresponding reduction of total flow (−3.8%), flow variance (−7.7%), peak flows (−4.7%), high flows (−7.6%), flashiness (−2.2%), and high flow frequency (−1.5%); and a corresponding increase in baseflow (4.3%). For a subset of these watersheds for which GSI data were available ($n = 48$), the level of GSI implementation showed a significant, but weak influence on urban greenness with a 20% increase in BMP density corresponding to a greenness increase of 0.9%. The study results may support valuation and verification of GSI co-benefits in urbanized landscapes at the watershed scale.

* Corresponding author.
E-mail address: gary@2ndnaturewater.com (G. Conley).

http://dx.doi.org/10.1016/j.scitotenv.2021.152723

1. Introduction

Increases in stormwater runoff caused by widespread expansion of impervious cover (Nowak and Greenfield, 2020) have detrimental impacts on water bodies, ranging from hydrologic regime alteration, erosion, and increased pollutant transport and loading (Arnold and Gibbons, 1996; Holman-Dodds et al., 2003; Walsh et al., 2005). Nature-based solutions, such as green stormwater infrastructure (GSI) mitigate the impacts of urban development on local hydrology and ecosystems, which have been extensively documented (e.g. Alberti et al., 2007). As a subset of structural stormwater control measures (SCMs), GSI reduces urban stormwater runoff and pollutant loading to waterways via processes such as infiltration and evapotranspiration to reduce, slow down, and clean urban runoff (Clary et al., 2002; Ebrahimian et al., 2019). GSI includes features such as green roofs, constructed wetlands, rain gardens, bioswales, and urban tree canopies, that are often widely dispersed throughout the urban landscape and commonly included as part of low impact development (LID) (Prudencio and Null, 2018). Urbanization has been shown to lead to shorter runoff lag times, higher total runoff volumes, and higher runoff peaks (Booth and Bledsoe, 2009; Shuster et al., 2005). GSI mitigate these hydrologic impacts by managing stormwater runoff close to its source (Berland et al., 2017) and disconnecting impervious cover (Ebrahimian et al., 2018). Where traditional “grey infrastructure” uses engineered hard structures, GSI uses plants, soils, and landscape design to infiltrate runoff and entrain pollutants to restore the natural hydrologic functioning of urbanized landscapes and improve water quality (Davis, 2007). GSI has become increasingly popular as a cost-effective way of reducing urban stormwater pollution (Wang et al., 2013); providing ecosystem services such as habitat protection, air quality improvements, and carbon dioxide (CO_2) uptake; and enhancing social well-being via recreational opportunities and enhanced community aesthetics (McDonald, 2015). These benefits associated with GSI implementation are largely vegetation-related and often referred to collectively as GSI ‘co-benefits’ (e.g., Spahr et al., 2020) to distinguish them from the traditionally assessed benefits of runoff reduction, pollutant treatment, and flood risk reduction. Even with widespread policy shifts towards more sustainable urban development (e.g. Gunder and Hillier, 2016; Fitzgerald and Laufer, 2017), cities still show widely ranging levels of GSI adoption and diverse implementation trajectories (Hale, 2016), with GSI performance uncertainty cited as a key barrier to mainstream adoption (McPhillips and Matsler, 2018). Indeed, an effective shift towards including more GSI in conjunction with grey stormwater management may depend on identification of appropriate metrics to demonstrate the value of GSI implementation over time (Chini et al., 2017).

The efficacy of GSI for runoff reduction and water quality improvement has been widely documented at the scale of individual BMPs and parcels (Ackerman and Stein, 2008; Clary et al., 2002; Strecker et al., 2004), but there is little compelling evidence available of improvements at the scale of urban watersheds (e.g., 1–1000 km^2) (Golden and Hoghooghi, 2018). While recent studies have begun to build an understanding of the impact of GSI on watershed-scale hydrology via empirical measurements (e.g., Ahiablame et al., 2013; Loperfido et al., 2014; Pennino et al., 2016), most studies rely on modeling experiments (e.g., Avellaneda et al., 2017; Kong et al., 2017). Results from direct measurements of effectiveness are mixed (e.g., Jarden et al., 2016); and substantial uncertainty remains for how implementation may scale up to watershed-scale changes over the long term (Sarkar et al., 2018; Vogel et al., 2015), largely to the confounding effects of hydrologic variability (Roy et al., 2014). For example, increases to the density and coverage of urban tree canopy reduces stormwater runoff impacts, along with providing various other ecosystem services (Selbig et al., 2021; Berland et al., 2017; Carlyle-Moses et al., 2020). But as with other types of GSI, current understanding of the aggregate, watershed-scale hydrologic changes associated with urban tree planting leaves much room for improvement (Coville et al., 2020). Experimental designs that provide a robust accounting for watershed factors that contribute to hydrologic variability have the best chance to draw causal linkages between GSI and catchment-scale hydrologic changes (Jarden et al., 2016). Yet most studies have relied on limited data using a paired watersheds approach (e.g., Dietz and Clausen, 2008; Hager et al., 2013; Roy et al., 2008; Yang and Li, 2013), which can have severe limitations for detecting differences, especially when treatment levels are low and time extents are short (Loftis et al., 2001). As a result, direct empirical data that support watershed-scale system responses to GSI remain scant.

Since GSI implementation can result in localized greening of the urban landscape, there is the potential to measure those changes at the urban watershed scale via spectral vegetation indices, such as the Normalized Difference Vegetation Index (NDVI), and to identify relationships between NDVI and the hydrologic benefits associated with urban greening. Hydrologic condition improvements related to GSI include reduction of local flooding risks (Tao et al., 2017; Venkataramanan et al., 2020; Zellner et al., 2016), recharging groundwater (Bhaskar et al., 2018; Dussaillant et al., 2005), and modulation of flashy runoff response (Fahy and Chang, 2019). While NDVI has been shown to be a useful proxy for other GSI co-benefits (e.g. Kanniah et al., 2014; Rani et al., 2018; Nieto et al., 2015), questions persist as to whether the NDVI may be similarly useful as a proxy for hydrologic condition improvements.

Despite the scale of investment in GSI implementation, only a few studies to date have quantified relationships between GSI and urban greenness, between GSI and hydrologic measurements, or have considered all of these factors together across a wide range of urbanized watersheds. The fact that the majority of evidence for the influence of GSI on hydrology has come from modeling scenarios (e.g., Fahy and Chang, 2019; Hoghooghi et al., 2018), rather than flow measurements, is due in part to a lack of appropriate gauged watersheds, and partly due to poor accessibility and harmonization of GSI data across the implementing entities. A notable exception is the study by Pennino et al. (2016), who identified weak but significant effects of GSI implementation on several downstream hydrologic and water quality metrics for three U.S. cities. There also does not appear to be strong consensus in the recent literature regarding urban greenness trends. While Corbane et al. (2020) found that most cities around the world are getting greener (1990–2014), Spahr et al. (2020) found that greenness was increasing in only two of 10 U.S. cities (1990–2015). Key questions remain surrounding urban greenness trends, the capacity to reliably measure the hydrologic effects of GSI, and whether the combined effects of increasing urbanization and urban greening policies may result in offsetting patterns of urban greenness within the same areas (Gan et al., 2014).

The potential to use NDVI measurements to quantify urban greenness changes and provide a proxy measurement to track GSI co-benefits are clear, and other researchers have called for decision makers to incorporate NDVI data to their planning processes to incentivize urban greening (e.g., Spahr et al., 2020). A fundamental precursor to development of urban greenness tracking metrics includes a better understanding of how well widely available satellite data measures urban greenness, what changes in land cover or GSI implementation are associated with greenness changes, and how urban greenness changes affect downstream hydrology. In this study, we explored changes in urban greenness patterns from 1985 to 2019 within urbanized watersheds across the United States (U.S.) We employed cloud-based spatial data processing tools and a panel regression statistical approach that allowed simultaneous exploitation of information contained in both spatial and temporal patterns of the data. Our objectives were to 1) identify urban greenness changes over time from satellite remote sensing data, 2) assess the impact of urban greenness on downstream hydrology, and 3) assess the impact of GSI implementation on both urban greenness and hydrology.

2. Data and methods

The study objectives were addressed via trend testing and regression modeling, with daily streamflow data used to measure hydrologic responses, and satellite NDVI data used to quantify urban greenness. Several watershed attributes and climatic variables were used as explanatory variables to account for watershed responses unrelated to anthropogenic changes or the predictor variables of interest (urban greenness and GSI implementation). Data development relied heavily on the use of Google Earth Engine (GEE; Gorelick et al., 2017) for acquisition and processing of large raster datasets spanning many individual years (1985–2019).

2.1. Study watersheds and attributes

Study watersheds were selected on the basis of USGS streamflow data availability (GAGES; Falcone et al., 2010) and proportional impervious coverage as defined by the National Land Cover Database (NLCD; Homer et al., 2020). Potential watersheds were filtered using two criteria: 1) >5% NLCD impervious coverage in the watershed in 2016, and 2) two-thirds of the years from 1985 to 2019 having <10% missing streamflow data. For watersheds with nested streamflow gauges, we selected the one with the highest proportion of impervious cover, so that there were no overlapping watersheds. This filtering process resulted in a total of 372 watersheds distributed across the U.S. (Fig. 1) representing a wide range of hydroclimate conditions and environmental regulatory regions (see Table S1, supplementary material).

Watershed predictor variables that are understood to strongly influence the rainfall-streamflow relationship at the annual time step were summarized for each watershed for each year for time-varying attributes. These included drainage area, precipitation, temperature, potential evapotranspiration, urban extent, and urban greenness. Precipitation (PPT) totals were calculated from gridded 24-hour event depths (4-km resolution) provided by the PRISM Climate Group (Daly et al., 2008) with depths summed for each grid cell (30 m) and an area-weighted average calculated for each grid cell that intersected watershed boundaries. Average annual potential evapotranspiration (PET) estimates were summarized from MODIS, 8-day measurements at 1-km resolution for the study period (Mu et al., 2013, 2011). We calculated the urban extent for each year based on the global artificial impervious area (GAIA) data product (Gong et al., 2020) that combines Landsat platform data with ancillary datasets including nighttime light data and the Sentinel-1 Synthetic Aperture Radar data. These data track the year of transition to >50% impervious cover for each pixel. The cumulative sum of impervious pixels each year provides a fine time-resolution measure of the expansion of urban extents over time. This dataset has the advantage of yearly resolution, compared to the NLCD impervious cover data products which are made available on a 5-year schedule.

Compared to other regression approaches, panel regression is more likely to avoid multicollinearity issues in identifying hydrologic effects of anthropogenic landscape change through simultaneous use of information across watersheds and over time (Steinschneider et al., 2013). While exploratory analysis showed moderate to strong correlations between some predictor variables (e.g., Temperature and PET), the panel modeling approach substantially reduces the risk that the model will be unable to identify the effect of an independent variable. Our general approach follows that of Steinschneider et al., 2013, who showed that the separate attribution of variability across both space and time dimensions in panel models can provide superior identification of hydrologic response characteristics that are generalizable across watersheds, and that panel models could isolate heterogeneity between watersheds caused by omitted predictors. Predictor variables used in the panel regression models are defined along with the flow response variables, and the urban greenness metric (described in Section 2.3) in Table 1.

2.2. Streamflow data

Mean daily discharge data were downloaded from the U.S. Geological Survey, quality checked, and processed using the R statistical programming software (De Cicco et al., 2018; R Core Team, 2018) for the period 1985–2019. For each station, a set of hydrologic metrics were calculated to represent various elements of streamflow regimes that may be affected by urban greenness changes or GSI. Flow metrics were calculated for each watershed for each year and included total flow, baseflow, flow variance, high flows, high flow frequency, peak flows, peak flow duration, and flashiness (Table 2). These metrics are similar to those used by Pennino et al. (2016), who found them responsive to GSI implementation. Baseflow was calculated using the Lynne-Hollick filter method through the hydrostats R package (Bond, 2015; Lyne and Hollick, 1979), while other hydrologic metrics were calculated manually as described in Table 1.

Daily flow data were used because the instantaneous flow data (15-min intervals) were only available for a subset of the study watersheds. To evaluate the impact of using the daily (rather than 15 min) data on the calculated flow metrics, we calculated the metrics for three watersheds located each of the three ecoregions representing the range of watershed sizes. Total runoff, baseflow, flow variance, and high flow days had strong relationships between the 15 min and the daily data (R-squared 0.75–0.99), while flashiness, peak flows, and peak flow duration showed moderately strong relationships with the 15-minute data (R-squared 0.41–0.54). For all metrics, there was <20% bias in the relationships indicating that the danger of introducing systematic offsets due to sub-daily flow variation

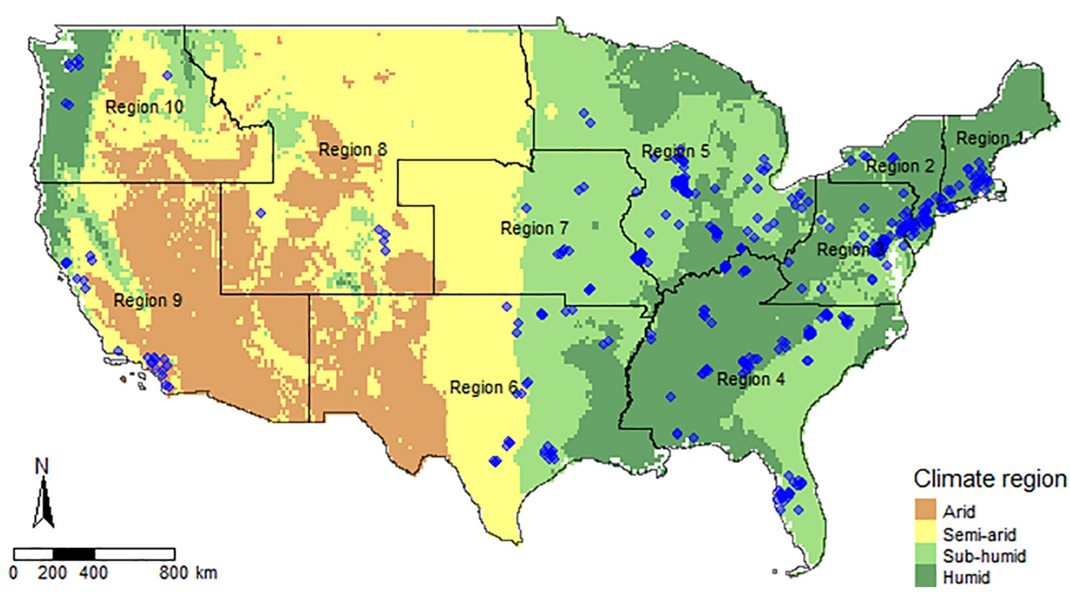

Fig. 1. Study watershed locations (blue dots), U.S. Environmental Protection Agency (EPA) regions, and climate regions based on aridity index (Cherlet et al., 2018), classified as quartiles. (For interpretation of the references to color in this figure legend, the reader is referred to the web version of this article.)

Table 1
Watershed response and predictor variables. Each variable is calculated for each watershed for each year in the time series (1985–2019).

Variable	Notation	Description	Units
Response variables			
Total runoff	Q	Total runoff	m^3
Baseflow	Qb	Mean daily baseflow	m^3/s
Flow variance	Qcv	Coefficient of variation for daily flows	%
High flows	Qhi	Mean flow > 3× monthly median flow (full time series 1985–2019)	m^3/s
High flow frequency	QhiDays	Count of high flow days > 3× monthly median flow (full time series 1985–2019)	days
Peak flows	Qpeak	Mean flow > 15-day median flow (current year)	m^3/s
Peak duration	QpeakDur	Mean number of consecutive days > 15-day median flow (current year)	days
Flashiness	QpeakRatio	Peak flow/15-day median flow	%
Predictor variables			
Drainage area	A	Watershed drainage area	km^2
Precipitation	PPT	Total precipitation	mm
Temperature	T	Mean temperature	°C
Potential evapotranspiration	PET	Total potential evapotranspiration	mm
Urban extent	UrbExt	Impervious pixel count	km^2
Urban greenness	UrbGrn	90th percentile NDVI value (current year)	NDVI

was low. Since the 15-minute data would have substantially reduced the number of watersheds that could be included in the study, using the daily flow data was the preferable alternative.

2.3. Urban greenness data processing

Greenness of the study watersheds was characterized using NDVI, which is widely used to estimate surface vegetation greenness and is calculated as a ratio of the red (RED), near-infrared (NIR) reflectance ratio [NDVI = (NIR − RED)/(NIR + RED)]. NDVI values thus range from −1 to +1, where negative values correspond to an absence of vegetation (Myneni et al., 1995). We used a combination of the Landsat data archives (USGS, 2020) and processing and analysis methods available via GEE (Gorelick et al., 2017). We created an NDVI time series using Tier 1 Surface Reflectance data from Landsat 5 Thematic Mapper (TM), Landsat 7 Enhanced Thematic Mapper Plus (ETM+), and Landsat 8 Operational Land Imager (OLI) sensors for years 1985–2011, 2012, and 2013–2019, respectively. Standard cloud and shadow masking procedures were used to prepare the Landsat imagery for analysis (Zhu et al., 2015). Water, snow, crop and pastureland cover types, classified by the 2016 NLCD land cover database (Homer et al., 2020), were also masked out of the imagery to remove effects attributed to agricultural practices or associated with water reflectance, although these land cover types were minimal within the modern urban boundaries. We used the prepared surface reflectance composites to calculate the 90th percentile value of the NDVI for each year (1985–2019) so that each pixel location retained only the 90th percentile value. The annual 90th percentile NDVI value was used to measure greenness levels, while avoiding data errors associated with the using the maximum NDVI value (e.g., striping errors that could not be removed with masking and other reflectance anomalies) and minimizing cloud cover effects that were not removed in the cloud masking process.

Annual 90th percentile NDVI raster outputs were averaged by area for the modern urban boundary of each study watershed producing a single aggregate urban greenness value for each watershed and each year. The modern urban boundary within each study watershed was defined from the 2016 NLCD impervious coverage data 1) with a 900-m focal median filter applied to impervious pixels to ensure that the defined urban footprint included open spaces within cities but did not extend into wildlands surrounding cities and 2) with any pixel > 0% impervious surface cover. In comparisons with the data from census blocks, municipal boundary datasets, or the global human settlement layer (Melchiorri et al., 2018), this method provided a better representation of the current urban footprints for the purpose of this study and also allowed inclusion of highways, which may also undergo designed greening (Li, 2015). To examine patterns of greenness change over the study period, we created an NDVI change layer, in which we calculated the difference between the average 90th percentile NDVI pixel values of the first three years of the time series (1985–1987) and the average pixel values of the last three years of the time series (2017–2019).

Improvements to the OLI sensor array over the previous TM/ETM+ sensors result in differences in spectral response, with the OLI showing consistently higher NDVI values than ETM+, requiring sensor intercalibration (Chastain et al., 2019; Mancino et al., 2020). Since NDVI emphasizes the difference between the red and near infrared bands, small differences in these bands may result in much larger differences in the NDVI, particularly in low vegetation areas (Miura et al., 2000). To mitigate this effect, we applied the widely used empirical regression equations reported in Roy et al. (2016) for OLI and TM/ETM+, but still saw clear evidence of a sensor-based NDVI offsets when examining data from ETM+ and OLI for overlapping years (2013–2019). We used the overlapping time period from 2013 to 2019 for ETM+ and OLI to create an empirical relationship based on the aggregate NDVI data (area-averaged annual 90th percentile NDVI by watershed). The resulting regression equation used to harmonize the NDVI data across the sensors was ETM+ = 0.049 + 0.978 ∗ OLI.

2.4. GSI data

A total of 204 stormwater programs with National Pollutant Discharge Elimination System (NPDES) permits within the study watersheds were contacted to request access to data on SCMs, which resulted in a total 44 programs providing data for the study. From these data, we could verify total watershed data coverage for 48 of the 372 study watersheds, drawn from 17 stormwater programs (see Table S2), with most jurisdictions spanning multiple watersheds. Restricting the analysis to those watersheds with full-area SCM data coverage facilitated meaningful comparison of the levels of implementation across these 48 watersheds. The level of detail and completeness associated with these data ranged widely, with the critical data fields required for our analysis being SCM type (e.g. dry basin, bioretention), location, implementation date, and drainage area. Datasets were rejected if the documented SCMs did not specify types, specific

Table 2
Streamflow response panel model results. Urban greenness coefficients, F-statistics, and *p*-values are estimated for each flow response model with coefficients in units of the response variables (see Table 1).

Response variable	R-sqrd	Adj R-sqrd	F-statistic	Model p-value	Significant predictors ($p < 0.05$)	UrbGrn coefficient	UrbGrn p-value
Total flow	0.178	0.150	471	<0.001	PPT, UrbGrn	−49,055,634	0.024
Baseflow	0.078	0.046	183	<0.001	PPT, UrbGrn	0.60	0.003
Flow variance	0.018	0.016	40	<0.001	PPT, PET, Temp, UrbExt, UrbGrn	−250	<0.001
High flows	0.053	0.019	117	<0.001	PPT, PET, Temp, UrbExt, UrbGrn	−10.9	<0.001
High flow frequency	0.123	0.093	305	<0.001	PPT, PET, UrbGrn	−12.5	0.001
Peak flows	0.221	0.194	611	<0.001	PPT, PET, UrbExt, UrbGrn	−5.59	0.002
Peak flow duration	0.116	0.085	282	<0.001	PPT, PET, Temp, UrbExt	−0.15	0.33
Flashiness	0.044	0.010	98	<0.001	PPT, PET, UrbExt, UrbGrn	−0.12	<0.001

locations (coordinates), or have at least two-thirds of the implementation dates recorded. To facilitate the regression analysis, missing dates within the non-rejected datasets were imputed by assigning a random implementation date within the study period. This approach assumed linear implementation of SCMs over the study period which reflected the aggregate implementation trajectory of all SCMs with dates reported. SCM types were harmonized based on the data records and ancillary documentation to clarify SCM typology. All SCMs were categorized in terms of whether or not they were expected to influence runoff volumes and whether or not they were vegetated, with GSI as a subset of all runoff-reducing SCMs with a vegetated component. Categorization of SCMs was based on their specified types (e.g. detention basins, treatment vaults, media filters, permeable pavement) and other documentation when available, with most of the SCMs (74%) coded as GSI (e.g. bioretentions, bioswales, wet basins, dry basins). Only a few of the SCM datasets provided by cities included urban tree planting inventories, and so they were excluded from our GSI dataset for consistency across watersheds. Since most of the data did not have drainage areas recorded for SCM features, implementation levels were quantified as the number of features per area of urban extent within each watershed. While the SCM data used in this study are unpublished and not available online in most cases, they may be available directly from the municipal stormwater programs, which are listed in supplemental materials (Table S2, supplementary materials).

2.5. Data analysis

2.5.1. Testing for urban greenness trends

We tested for urban greenness trends over the study period (1985–2019) using the non-parametric Partial Mann-Kendall (PMK) test (Libiseller and Grimvall, 2002), implemented in R via the 'trend' package (Pohlert et al., 2016). This approach allows direct incorporation of covariates to the trend test to improve trend detection power (Bromssen and Grimvall, 2002). Trend magnitude was quantified using the Sen slope estimator (Sen, 1968). Removal of the climatic signal of greenness variation is an essential first step towards measuring greenness change is associated with anthropogenic factors. More than 50% of the study watersheds had significant trends in either precipitation or temperature or both. Exploratory data analysis showed that watersheds located in the West and Southwest areas of the U.S. had the lowest average urban greenness, and also had the strongest positive correlations with precipitation, which aligns with the relationships reported in the literature (Burrell et al., 2017). Temperature had an overall negative correlation with urban greenness, also reflecting the strong influence of the warm, arid and semi-arid regions. To account for these factors, we tested trends on the residuals from a linear model that used urban greenness as the response and precipitation and temperature as explanatory variables. The PMK trend tests used yearly urban extents as covariates, so that the greenness trend tests accounted for the growth of urban footprints over time, similar to the approach employed by Corbane et al. (2020), so that the greenness trends reflected greenness changes per unit area of urbanized watershed.

2.5.2. Panel regression modeling

To quantify the influence of urban greenness on downstream hydrology, we used a panel regression approach, implemented in R, using the *plm* package (Croissant and Millo, 2008). Panel regression has been widely used in econometrics, and while the estimated models can be more informative and improve capacity for detecting the effects of anthropogenic changes, this method has rarely been applied to hydrologic studies. Previous work has shown that panel regression may be a more appropriate method compared to cross-sectional or time series analyses for describing relationships between landscape changes and hydrologic responses, and that response detection is strongly dependent on the data dimensions and model structure (Steinschneider et al., 2013). By pooling multidimensional data across watersheds and through time, panel regression can identify response characteristics unique to individual watersheds and those common across watersheds. It draws on the strengths of the two most common approaches for hydrologic studies, longitudinal and cross-sectional analysis, combining them both into a single regression framework. Panel regression can provide more efficient model parameter estimates with the increased degrees of freedom that comes from concurrent consideration of all data through time and across watersheds; simultaneous accounting of confounding variables that vary over time and strongly influence hydrologic responses, such as climate variables; and a means to account for unobservable (or poorly observed) heterogeneity across watersheds (Steinschneider et al., 2013). In this study, the panel regression approach is used to describe relationships between urban greenness, hydrology, and GSI via the modeling experiments described in the following sections.

2.5.3. Effect of urban greenness on hydrology

To build the panel regression model to assess the impact of urban greenness on downstream hydrology, we used the entire dataset of 372 watersheds with the eight hydrologic metrics (described in Section 2.2) and each predictor variable averaged for each urban boundary, for each year of record over the study period. The hydrologic metrics were used as the response $Q_{i,t}$, which were assumed to be random variables, and observed over the study period T at each annual time step (t) for each watershed (i). The set of predictors (K) are urban greenness, rainfall totals, temperature, PET, drainage area, and urban extents, and are assumed to be fixed in random sampling, represented as $X_{i,t} = \{x^1{}_{i,t}, x^2{}_{i,t}\ldots, x^k{}_{i,t}\}$. Thus the general formulation of the panel model can be expressed as in Eq. (1).

$$Q_{i,t} = \beta_0 + \mu_i + \sum_{k=1}^{K} \beta_k \times x_{i,t}^k + \varepsilon_{i,t} \quad (1)$$

where β_k is an unknown response coefficient that quantifies the influence of the $x^k{}_{i,t}$ predictor on the flow response variable $Q_{i,t}$ in the ith watershed at time t, β_0 is the mean intercept for all watersheds, μ_i is the watershed specific time-averaged differences in the flow variable between watersheds, and $\varepsilon_{i,t}$ is the random error term with constant variance and an expected value of 0. The predictor variables are used to account for variability in hydrologic responses within a watershed over time, as well as the variability between time-averaged hydrologic responses. Since we have selected our study watersheds on the basis of urbanization, there may be unobservable factors that cause heterogeneity across watersheds to be correlated with other variables in the design matrix. In this situation, while the fitted parameter estimates of a random effect model may be inconsistent due to correlation with components of the design matrix, a fixed effects model is expected to produce consistent estimators (Steinschneider et al., 2013). Appropriateness of the fixed effects model specification was verified via a Hausman test (Hausman, 1978) calculated within the *plm* R package. We tested for spatial correlation in the model residuals using Moran's I test for residual spatial autocorrelation included in the *spdep* package, also written in R (Bivand and Wong, 2018).

2.5.4. Effects of GSI on urban greenness and hydrology

In addition to measuring the effect of urban greenness on hydrology, we were also concerned with causes of urban greening and whether GSI (and SCMs in general) have a direct measurable effect on watershed streamflow. This portion of the study was constrained to the subset of 48 watersheds with a complete SCM dataset to allow meaningful comparisons across watersheds. The first analysis consisted of 2 sets of estimated panel models to identify the effect of SCM or GSI implementation on the eight hydrologic response variables (16 models total). SCMs and GSI were each specified as separate independent variables in their own sets of models, since GSI is a subset of all runoff-reducing SCMs with a vegetated component. The second analysis required estimation of only a single panel model to identify the influence of GSI implementation on urban greenness, since urban greenness was the only response variable considered. For both sets of analyses, other predictor variables included precipitation, PET, drainage area, and urban extent. Like the previously described panel models, we specified fixed effects models with the general form described in Eq. (1).

3. Results

3.1. Urban greenness trends

Residuals from the linear model with precipitation and temperature used as independent variables represent the climate-adjusted urban greenness values, which are shown across the study period in Fig. 2A. Most watersheds showed significant urban greenness trends using the climate-adjusted urban greenness (271of 372 watersheds), the majority of which were negative (167). The negative NDVI trends were likely related to the expansion of the urban footprints within the study watersheds over time. Given that there were also 104 positive trends, an aggregate trend across watersheds is not discernable in Fig. 2A. Fig. 2B shows the aggregate trend in the growth of urban extents over time. Because the trend test uses the climate-adjusted urban greenness values within the modern urban boundary, these negative trends at least partially reflect the progressive filling up of that boundary by urban cover that can reduce the average greenness of pixels. Thus, by accounting for the annual change in urban extents over time, this greenness trends analysis reflects greenness changes per unit area of urbanized watershed, irrespective of how much cities have expanded across the study period.

Stage-wise regression procedures can be less powerful and misleading when covariates are linearly dependent on time, since part of the human induced trend may be attributed to changes in the covariates (Smith and Rose, 1991). Libiseller and Grimvall (2002) report that the PMK test (which includes a single covariate) is most useful when there are either time-delayed effects or when an influencing variable exhibits a long-term trend. Since the urban extent showed the strongest aggregate trend over time (compared to precipitation and temperature) and a consistent positive trend direction across watersheds, this variable was incorporated directly into the PMK trend test as a covariate that is partialled out (directly accounted for) in the test for trend.

After accounting for the influence of precipitation, temperature, and urban extent, we identified significant urban greenness trends in 32 out of 372 urbanized watersheds (9%). Significant results ($p < 0.05$) are mapped in Fig. 3, with color indicating direction and magnitude via the Sen slope estimator. Ten watersheds showed increasing urban greenness over the study period (1985–2019), while 22 showed decreasing urban greenness. Trend magnitudes ranged from -0.0021 NDVI/year to 0.0019 NDVI/year, which translates to a change of approximately ± 0.07 NDVI over the 35-year study period, which is similar in magnitude to annual seasonal shifts in the NDVI within the urban boundaries. Most of the significant trends are in the eastern part of the U.S., which reflects the greater number of study watersheds in that region (see Fig. 1). We detected both increasing and decreasing trends across climate regions with no consistent correspondence between trend magnitude or direction and climate region, watershed size, or urban extent.

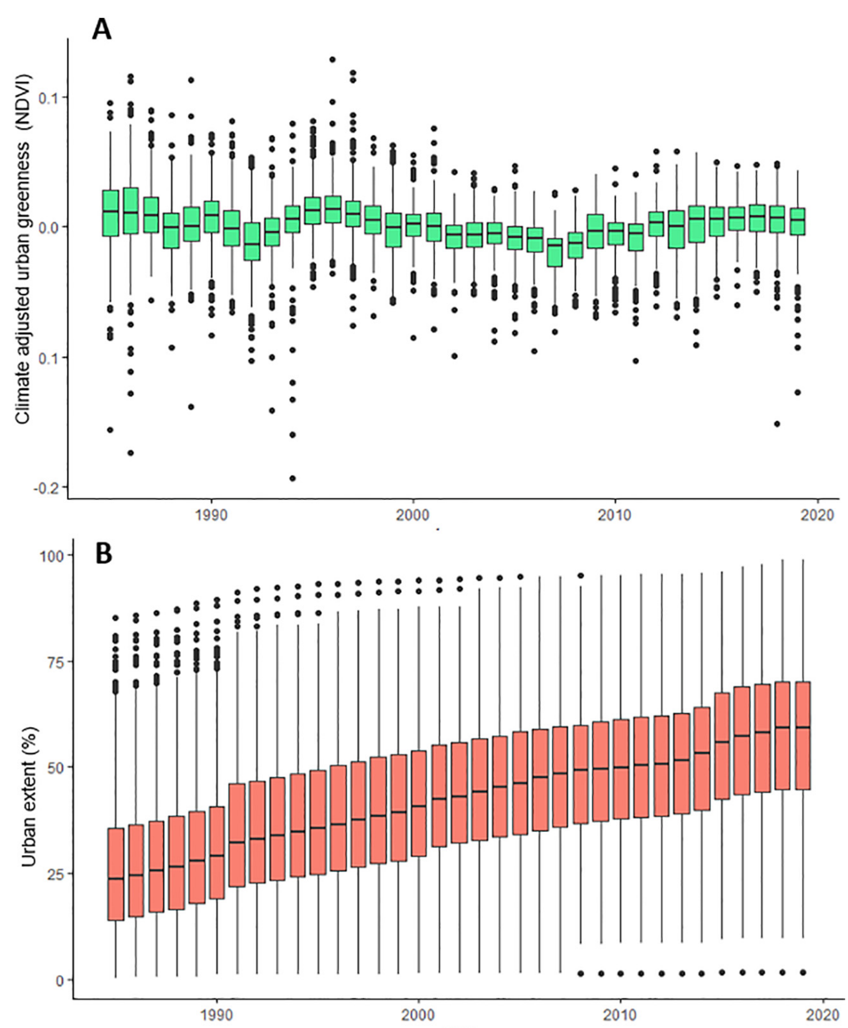

Fig. 2. Box plots of urban greenness (A) and urban extent (B) over the study period (1985–2019) for all study watersheds ($n = 372$). Boxes show median values and the interquartile range, whiskers show 1.5× the interquartile range, and dots are outlying points. Urban greenness is defined by the 90th percentile Normalized Difference Vegetation Index (NDVI) value for each year, averaged for each urban boundary.

Visual inspection of urban boundaries with significant trends indicated that the land cover changes were largely located in outlying areas of cities, indicating that the significant trends may be associated with new development, rather than redevelopment and replacement of existing impervious coverage within the central core of cities. Fig. 4A illustrates an example of a watershed outside of Minneapolis, MN with increasing greenness, which appears to be largely due to the maturation of tree canopies during the study period. Greening in the ten watersheds with increasing trends was typically associated with tree canopy maturation in the outlying urban areas. Inspection of several watersheds indicated that changes to the urban extents were accurately reflected in the urban extent variable, meaning that the expansion was accounted for as a covariate in the PMK trend test. This means that a positive trend indicates that these areas are greener per new area of urbanized watershed, which in some watersheds is likely driven by less dense residential developments at the perimeters of cities. Several of these neighborhood-scale changes contribute to the more clustered appearance of the positive trending urban greenness change map (Fig. 4A) compared to watersheds with an overall negative greenness trend (Fig. 4B). In the typical watershed example with a negative urban greenness trend, pixels showing change represent development of small open spaces that persisted within the urban boundary for some span of the study period, such as the fallow field shown in Fig. 4B that was converted to a parking lot after 1994.

3.2. Effects of urban greenness on hydrology

Panel modeling results that included 372 watersheds across the study period (1985–2019) are provided in Table 2. Each of these models included the drainage area, precipitation, temperature, potential evapotranspiration, urban extent, and urban greenness as explanatory variables. All models were significant at the 99.9% confidence level ($p < 0.001$), except for the peak duration model, and explained approximately 1–19% of variance in the flow response variables per the adjusted R-squared value (Table 2). Urban greenness had a significant effect ($p < 0.05$) in seven of the hydrologic response models, with total flow, flow variance, high flows, high flow frequency, peak flows, and flashiness all being reduced with increasing greenness; and baseflow showing an increase with greater urban greenness. While there are likely hydrologically relevant variables unaccounted for in these models contributing to the high unexplained variance (e.g. watershed slope, aspect, permeability, flow regulation), R-squared values are generally low in cross sectional data compared to time series due to greater heterogeneity of factors over cross-sections (watersheds). Even though the R-squared values reported in Table 2 are low, all of the regression slope coefficients are significantly different from 0 ($p < 0.05$), indicating that these models have statistically significant explanatory power for the flow responses. Since the intent of the model is to be explanatory rather than predictive, the significance and estimated coefficients for the urban greenness predictors contain the most relevant information for our purposes. With seven of the eight hydrologic response models showing significant urban greenness coefficients, the direction of the coefficient signs indicate that urban greenness attenuates some of the hydrologic impacts typically associated with urbanization.

Since the panel model includes no higher order terms or interaction terms, the urban greenness coefficients can be interpreted directly in terms of unit changes in the response variables. Mean changes in the flow metrics are shown in Fig. 5 for a range of urban greenness change increments. Six of the eight flow response variables showed negative changes with increasing urban greenness. On average, we would expect a 10% greenness increase to be associated with reductions to total flow (−3.8%), flow variance (−7.7%), peak flow volumes (−4.7%), high flows (−7.6%), flashiness (−2.2%), high flow frequency (−1.5%); and a corresponding increase in baseflow (4.3%).

The strongest effects of urban greenness within the panel models were the high flows and the flow variability. Reductions in these and other flow metrics match our conceptual interpretation of the role that vegetation increases have on watershed hydrologic processes: reducing runoff volumes and slowing runoff timing through increased interception and storage, and greater evapotranspirative losses. Only baseflow levels showed an increase with increasing urban greenness (Table 2), reflecting a greater proportion of runoff delivered more slowly rather than via hydrograph peaks. The baseflow increase represents the mirror effect of the flashiness reduction in response to increased greenness – a flattening of the streamflow hydrographs, with less annual runoff volume contained in the hydrograph peaks. The increase in baseflow with increasing urban greenness observed in these results is consistent with findings by Tan et al. (2020), who identified the same dynamic for more than 1000 watersheds across the globe located in both arid/semi-arid and humid/sub-humid regions.

3.3. Effects of SCM on hydrology and GSI on greenness

The compiled SCM datasets for 48 of the study watersheds covered nine states and six of the ten EPA regions in the U.S. Missouri had the highest

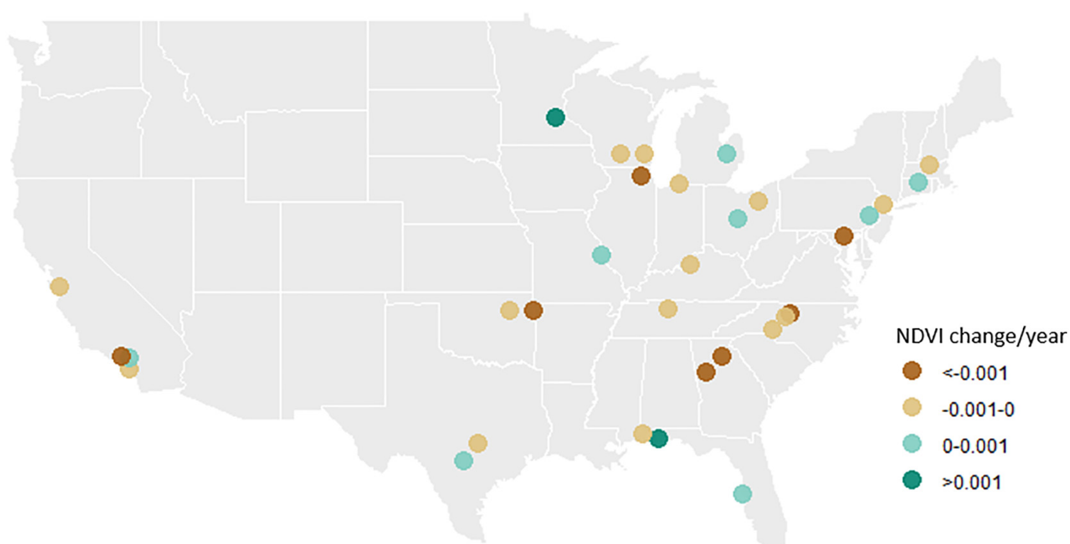

Fig. 3. Rates of urban greenness change for watersheds showing significant trends ($p < 0.05$) over the study period (1985–2019), with rates of change estimated via the Sen slope estimator (Sen, 1968). Urban greenness is defined by the 90th percentile Normalized Difference Vegetation Index (NDVI) value for each year, averaged for each urban boundary.

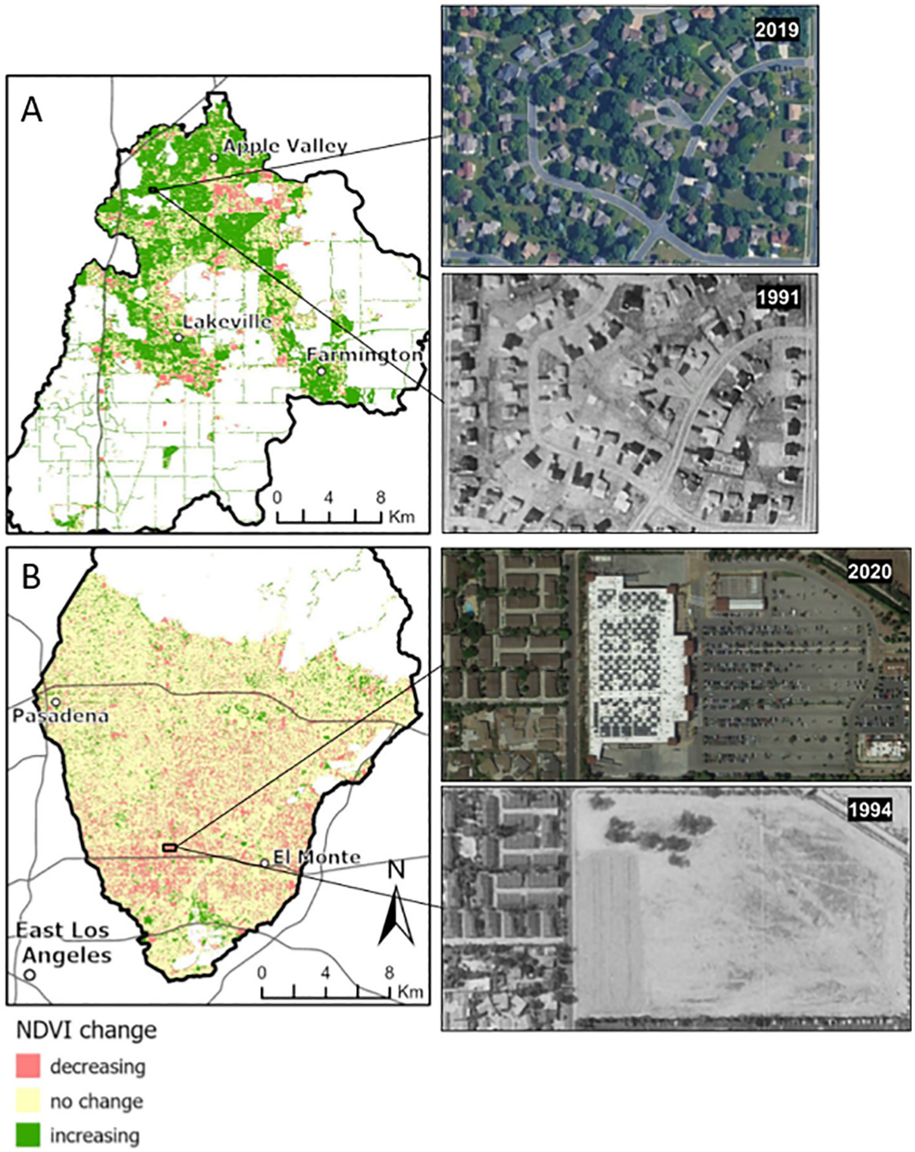

Fig. 4. Normalized Difference Vegetation Index (NDVI) change maps showing examples of an increasing greenness trend site near Minneapolis, MN (A) and a decreasing greenness trend site in Los Angeles, CA (B). Inset photographs show the same site at two different times in real-color (top of each pair) for the present and black-and-white (bottom of each pair) for the 1990s.

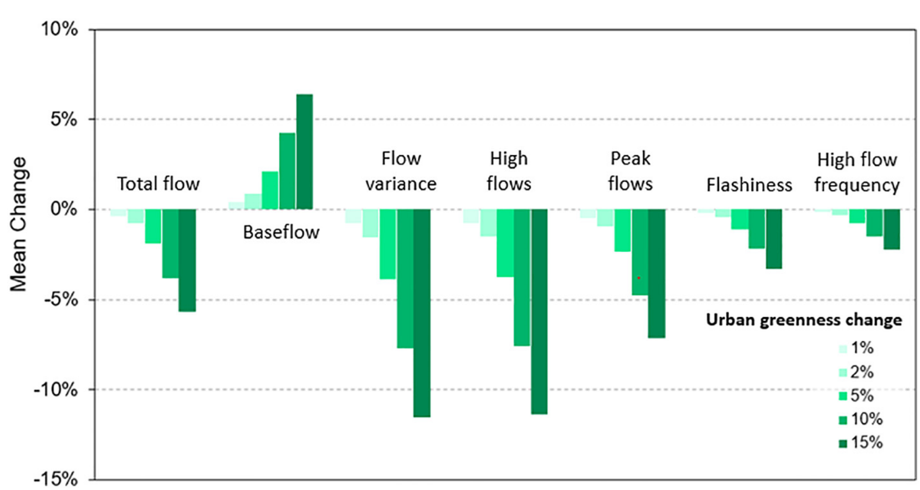

Fig. 5. Mean change in flow metrics per unit changes in urban greenness across all urban watersheds calculated using coefficients from the flow response panel models.

concentration of watersheds with SCM data, due to robust SCM tracking by the Metropolitan St. Louis Sewer District and a high density of gauged urban watersheds in that region. Present-day implementation densities of SCMs with runoff reduction benefits ranged from 0.66 features per km^2 to 74.53 features per km^2 with a mean of 6.77 features per km^2 within individual watersheds. Across hydroclimatic regions, average GSI counts were 0.6 features per km^2 in arid areas, 15.1 features per km^2 in humid areas, 6.2 features per km^2 in semi-arid areas, and 4.1 features per km^2 in sub-humid areas Densities of the GSI SCMs were on average 17% lower than non-vegetated SCMs. GSI implementation trajectories over time showed nearly constant rates of implementation for many watersheds, though several watersheds had an acceleration of implementation levels beginning around the year 2000.

Of the 16 panel models estimated to investigate the influence of GSI/SCMs on the streamflow variables, none showed either GSI or SCMs to be significant predictors of hydrologic responses, so that the F-statistics for GSI and SCM variables both had p-values > 0.05. Since these models included the same covariates as the previous analysis (with the exception of urban extent), all of the models explained a significant, albeit low, proportion of variance in the hydrologic responses (results not shown). Thus, contrary to our expectations based on previous work (e.g., Pennino et al., 2016), our results do not provide direct evidence of the influence of stormwater management measures (excluding tree canopy cover) on downstream hydrology.

The final analysis explored the influence of GSI implementation on urban greenness using a panel model using urban greenness as the response variable, with the results presented in Table 3. The model terms PPT, PET, and GSI showed significance at the 99.9% confidence level, while Temp was below the 95% confidence level. GSI implementation showed a small but highly significant influence on urban greenness ($p < 0.001$). Signs of the model coefficients are oriented as we would expect from the previous trends analysis – positive for PPT, negative for PET; and in alignment with the greening effects of GSI. Like most of the models estimated for hydrologic responses, the urban greenness response model showed poor predictive performance, with an adjusted R-squared value of 0.16. Urban extent was not included as a separate factor in this model because it is the denominator used for calculating the GSI density predictor variable. We can interpret the significant GSI predictor with a positive coefficient to mean that within the domain of these data, watersheds/time periods with higher density of GSI implementation relative to their urban coverage tend to be greener than those with lower densities of GSI implementation. The model coefficients (Table 3) indicated a weak GSI effect on urban greenness, so that on average, a 20% increase in GSI feature density corresponded with an urban greenness increase of only 0.9%, which nonetheless represents a stronger effect than the other two terms in the model (PPT and PET).

4. Discussion

4.1. Urban greenness trends

Our rate of detection of significant greenness trends (9%) is lower than some recent studies. For example, Spahr et al. (2020) found significant greenness trends in six out of ten U.S. cities, with four negative and two positive trends (1990–2015). However, before our correction for the changing urban extents in the PMK analysis, our findings are remarkably similar to those of Spahr et al. (2020), with negative trends detected in 45% of watersheds and positive trends detected in 28% of watersheds. The difference between the two results seems to be in our accounting for change in urban extents over time, which Spahr et al. (2020) did not account for in their analysis, which reduces the number of both negative and positive trends. The two approaches address two subtly different questions – with the current study attempting to isolate the effect of *how* cities are expanding or redeveloping (e.g., greener or greyer) in proportion to the growth of urban cover within watersheds. Corbane et al. (2020) performed a similar accounting of urban footprint expansion over time using the GHS-BUILT dataset (Pesaresi et al., 2016) in a global study which found that most cities were getting greener from 1990 to 2016. This may have to do with a global greening trend attributed to CO_2 fertilization (Zhu et al., 2016), or it may be partly related to inter-sensor Landsat calibration. We found that the equations developed by Roy et al. (2016) to correct Landsat bands between TM/ETM+ and the OLI sensor (also used by Corbane et al., 2020) did not adequately correct for the reflectance differences in red and near infrared bands in urbanized watersheds. Even with the Roy et al. (2016) correction applied, we observed a clearly discernible jump in the NDVI with the onset of the OLI sensor, which prompted us to use an additional empirical correction derived from the aggregate NDVI datasets, similar to the approach used by Spahr et al. (2020). In terms of the spatial patterns of greenness changes, our findings correspond with those of Czekajlo et al. (2020), who identified losses in greenness for 16% of study areas concentrated in the high-density urban centers, with greenness increases (14%) prevalent in outlying, lower density areas.

Table 3
Panel model outputs to explain watershed greenness response. Test statistics and p-values denote significance of each predictor and coefficient values indicate effect direction and size.

Predictor variable	Coefficient	Std. error	t-value	p-value	R-squared	Adj. R-squared
PPT	2.39E−05	2.48E−06	9.63	<0.001	0.20	0.16
Temp	−2.27E−04	1.07E−03	−0.21	0.83		
PET	−5.72E−06	1.24E−06	−4.60	<0.001		
GSI	6.34E−04	1.64E−04	3.87	<0.001		

4.2. Relationships between urban greenness, hydrology, and GSI

Hydrologic effects of anthropogenic change can be extremely difficult to isolate given natural variability commonly observed in hydrologic data (Price, 2011). Our intent with the use of panel models in this analysis was to maximize capacity to differentiate between climate and anthropogenic signals with simultaneous consideration of variations over time and across watersheds, which has been effectively demonstrated by others (Blum et al., 2020; Steinschneider et al., 2013). The consistency of urban greenness as a significant predictor in the panel models, across an array of hydrologic responses, and alignment of the coefficient signs with our conceptual understanding of the hydrologic role of vegetation abundance in watersheds provides strong evidence of the influence of urban greenness on downstream hydrology. Similar to the panel model coefficient interpretation approach used by Blum et al. (2020), who found a 3.3% increase in floods for each percentage point increase in impervious cover, our panel model outputs illustrated the range of effects for various hydrologic responses per incremental change to urban greenness (NDVI). This result provides a good starting point for understanding how to value increased urban greenness in terms of restoring natural hydrologic regimes in urbanized watersheds that have undergone substantial alteration (O'Driscoll et al., 2010).

Panel models provide an advantage for dealing with both multicollinearity of predictor variables in hydrologic systems and difficult to observe factors that contribute to watershed heterogeneity such as aspect, shape, slope, subsurface geology, macroflow paths, soil hydrologic properties, impervious connectivity, stormwater infrastructure systems, and water resource management (Steinschneider et al., 2013). The levels of unexplained variance in the models relating urban greenness to hydrology indicate that in addition to urban greenness and the other explanatory variables quantified, one or more of these factors are important drivers of hydrologic responses at the scales explored in this analysis. Another factor contributing to that unexplained variance for some of the hydrologic responses may be related the use of daily streamflow data, which were the only data available for all study watersheds. Such impacts would have been exacerbated in smaller watersheds, where hydrographs may last fewer than 24 h. Omitted predictors may have also played a role in the significant effect of GSI implementation on urban greenness. Work by Spahr et al. (2020) indicates that areas adjacent to GSI installation, along with the lag between installation dates and vegetation maturity, play key roles in determining the greenness contributions of GSI. Factors that co-vary with GSI implementation over time or space, such as coincident maturing tree canopies, which seemed to strongly influence the greenness trends, may have also influenced the GSI-urban greenness relationship. However, stepwise model building showed that an interaction term between the urban extent and GSI implementation variables was not significant, indicating that GSI had a consistent influence across different levels of urban extent, and that significance of the GSI term is not solely a function of growing urban extents.

While the analysis showed clear evidence of both the association between urban watershed greenness and between GSI implementation and urban greenness, the direct connection between GSI implementation and hydrologic changes was not evident given the data and methods employed in this study. This may be either because the hydrologic influence of these features is very small relative to other unaccounted for sources of variation, or because the measurement of GSI implementation levels contains levels of uncertainty that confound the analysis. While most of the datasets did not have drainage areas associated with GSI features, those that did showed a median watershed coverage of only 8.7%. Given that hydrologic responses to watershed urbanization tend to be thresholded, rather than linear (e.g., Beighley and Moglen, 2002), the lack of significant effect for GSI influence on hydrologic responses may have been a manifestation of this effect– wherein a threshold of GSI implementation must be reached before any heterogeneity of implementation across watersheds or over time has any meaningful impact on watershed-scale hydrologic responses. In addition, the distribution of GSI implementation within watersheds, which we did not quantify, can affect hydrologic response to these features (Perez-Pedini et al., 2005). Our results on this topic do indeed appear to contrary to both modeling evidence (e.g., Fahy and Chang, 2019), and empirical measurements (e.g., Pennino et al., 2016) that demonstrate the efficacy of GSI to change downstream hydrologic conditions. The apparent conflict may be related to a poor capacity to consistently measure GSI implementation across many cities.

The quality of the GSI data likely had a greater impact on the outcome compared to the reduced number of watersheds (48) available for constructing the GSI models. A post-hoc power analysis performed using the G*Power tool (Faul et al., 2007) indicated that given the 1680 observations available to these models (each year-watershed combination representing a unique case), an alpha level of 0.05, and a small effect size (Cohen's $f^2 = 0.01$) (Cohen, 1988), the power for detecting a significant effect of the GSI coefficient is greater than 90%. In comparison, Pennino et al. (2016) found significant hydrologic effects, examining only four cities, but these cities were in relatively small watersheds (0.5–34 km^2) compared to the current study, and they were selected partly based on their abundance and quality of GSI implementation data.

4.3. GSI data synthesis challenges and opportunities

The lack of a significant effect of GSI implementation levels on hydrologic condition improvements for the models estimated in this study was at least partially attributable to the variable quality and completeness of the available GSI data. To our knowledge, the current study represents the most comprehensive synthesis of SCM/GSI data yet reported in the scientific literature and highlights the limitations on the utility of these data for analysis at regional or national scales. With only 13% of the study watersheds able to meet the minimum data standards we required for inclusion in the analysis, primary challenges included missing or incomplete GSI inventories, inconsistencies in GSI typologies and data standards, and lack of centralized and publicly available data repositories. Such issues are consistent with those identified in recent prior efforts (McPhillips and Matsler, 2018). Many city stormwater programs contacted for this synthesis effort did not have systems in place for tracking implementation, did not store associated spatial data, or did not have access to data or measures implemented by other city departments or on private property. The lack of consistent data standards resulted in a wide range of data formats and completeness, which required considerable effort to harmonize into a coherent dataset. Inconsistent and contradictory naming conventions across cities added uncertainty to the analysis, as did the common absence of key data fields such as treated area, volumetric capacity, footprint or construction date. It is clear from this effort that any analysis with the potential to provide compelling evidence of watershed-scale GSI effectiveness would benefit from concerted effort to adopt a nationally recognized SCM data standard. Previous efforts along these lines (e.g., Maestre and Pitt, 2005) will need to be redoubled in a way that is closely aligned with the objectives, data management capacity, and tracking needs of municipal stormwater programs.

4.4. Tracking urban greenness changes and GSI co-benefits

Accounting for vegetation-related benefits will require identification of the most appropriate measurement scales (both temporal and spatial) for tracking urban greenness changes and assigning credit for various practices. Aggregate, city-wide greenness changes may prove to be less informative compared to more localized changes that can be quantified by hot spot analysis (e.g., Spahr et al., 2020). Likewise, the 30 m pixel size of the Landsat NDVI is likely to be too coarse to reliably capture changes associated with many small-scale greening changes associated with GSI implementation as this resolution has even been shown to underestimate urban tree canopy coverage (Nowak and Greenfield, 2010). Other datasets, such as the U.S. Department of Agriculture's National Agricultural Imagery Program (NAIP; 1 m resolution), which provides at a resolution of 60 cm to 1 m (depending on image capture year), or European Space Agency's Sentinel missions (10 m resolution) may prove more useful for detailed tracking going forward. Given that increases to urban greenness are likely the result of a mixture of sizes and types of vegetation (Rugel et al., 2017) and context dependent (Spahr et al., 2020), precise assignment of the sources of greenness changes may require higher resolution data such as the NAIP imagery. However, the limited coverage, temporal extents, frequency, and/or band coverage of the NAIP and Sentinel datasets will be less useful for the type of historical analysis performed in this study. The NAIP imagery, for example, is acquired on three- or five-year cycles for the years 2003–2015, with NIR band only acquired 2007 and only for some US states. Another promising option recently explored by Czekajlo et al. (2020) for decerning urban greenness changes at higher levels of resolution over long-time frames is to apply spectral mixture modeling to disaggregate greenness fractions of the 30 m Landsat pixels.

Tracking long-term urban greenness changes can provide a way to measure progress towards improving the overall health and resiliency of urban landscapes (Ahern et al., 2014), the positive impacts of those changes on communities, and identify persistent patterns of racial/social inequity within cities (McDonald et al., 2021; Venter et al., 2020; Casey et al., 2017). While this study has focused on the role of urban greening for watershed-scale hydrologic improvements, a meaningful accounting of the value of increasing urban greenness should include a broad spectrum of environmental improvements (McDonald, 2015) and social welfare benefits (Wolf et al., 2020). Bell et al. (2019) describe the broad array of co-benefits associated with SCMs (hydrologic, environmental, and social well-being) and their relationships to both stormwater management processes and vegetation. In this context, the NDVI (or other satellite-derived vegetation indices) can be used to set urban greenness targets and verify progress to incentivize vegetated solutions via assignment of credit based on their contributions to these co-benefits. Reliable quantitative relationships between urban greenness changes and environmental co-benefits can provide a convenient means to track the value of GSI and integrate that accounting into stormwater planning. For example, Spahr et al. (2021) propose a framework for evaluating the value of SCM features inclusive of benefits such as improved air quality, CO_2 sequestration, urban cooling, neighborhood aesthetics, and recreational opportunities. These authors outline options for integration of GSI co-benefits valuation with modeling tools to estimate runoff reductions, water quality treatment, and flood risk mitigation. Such holistic decision support tools can provide a more meaningful accounting of the value of urban greening to communities and facilitate the assessment of cost trade-offs with traditional grey infrastructure solutions. Coupling co-benefit accounting systems with remote sensing-based greenness measurements can provide a means to verify progress towards urban greening goals and perhaps provide proxy measurements for GSI co-benefit quantification. As suggested by Spahr et al. (2021), this can allow cities to distinguish contributions to various co-benefits by different types and sizes of urban greening. Implementation of these concepts as a spatial decision support tool can help cities with project siting, assessing local logistical constraints and trade-offs, and identifying where greening projects can do the greatest good in historically underserved areas of cities.

5. Conclusions

After accounting for climate variables and the expansion of urban extents over time, 9% of our study watersheds showed significant trends over the study period (1985–2019), with approximately 3% showing increasing greenness trends. While this means that most cities have not undergone aggregate greenness changes relative to their size that are measurable from the Landsat data, it does not preclude localized changes to greenness patterns. Further work is warranted to identify the optimal spatial scales for tracking greenness changes in cities, as greenness changes at finer scales likely contributed to the reliable influence of urban greenness on watershed hydrologic responses. We detected the influence of urban greenness on downstream hydrology for seven out of eight flow metrics, providing strong evidence that greener urban settings have the potential to mitigate watershed-scale hydrologic impacts commonly associated with urbanization. The panel regression model coefficients provided a means for estimating expected hydrologic changes per unit of greenness change, illustrating how greater vegetation abundance affects hydrologic processes within an urbanized watershed - reducing the magnitude and quickness of flow responses to rainfall. These results provide an example of how urban greenness changes can be valued in terms of their measurable benefits for mitigating urban runoff impacts.

Building quantitative relationships between GSI implementation and ecosystem service co-benefits can improve the ability to account for and communicate the overall value of GSI implantation. Success will depend on identifying the most appropriate spatial scales for greenness tracking and upon accurate accounting of GSI implementation over time. GSI was a significant (although weak) factor for explaining urban greenness in the panel models. We were not able to detect the influence of GSI on downstream hydrology, but the approach was severely limited by a lack of complete and consistent GSI data across watersheds. Uncertainty associated with quantifying GSI implementation levels is partly due to the lack of a nationwide SCM/GSI data standard, which will likely continue to confound hypothesis testing related to the watershed-scale efficacy of these measures at regional or national scales. As the usage of GSI continues to grow, tracking the value of these investments is more critical than ever to justify expenditures, plan for the future, and overcome barriers to adoption. Future work will focus on how to fill key GSI data gaps, identifying the optimal remote sensing data for urban greenness tracking, and developing a practical approach for cities to use greenness metrics for a detailed accounting of the co-benefits associated with urban greening and GSI.

Supplementary data to this article can be found online at https://doi.org/10.1016/j.scitotenv.2021.152723.

CRediT authorship contribution statement

Gary Conley: Conceptualization, Methodology, Data analysis, Writing. **Rob McDonald**: Methodology, Writing. **Tyler Nodine**: Methodology, Data Analysis, and Visualization. **Teresa Chapman**: Methodology, Data Analysis, Writing - Reviewing and Editing. **Craig Holland**: Methodology, Writing - Reviewing and Editing. **Chris Hawkins**: Writing - Reviewing and Editing. **Nicole Beck**: Conceptualization, Supervision.

Declaration of competing interest

The authors declare no conflict of interest. The funders had no role in the design of the study; in the collection, analyses, or interpretation of data; in the writing of the manuscript or decision to publish the results.

Acknowledgements

Catherine Riihimaki provided valuable insights and comments in the production of this manuscript.

Funding

This research did not receive any specific grant from funding agencies in the public, commercial, or not-for-profit sectors.

Data and software availability

All software developed R for data analysis in the study is available via Github: https://github.com/thegaryconley/Urban-Greenness.

References

Ackerman, D., Stein, E.D., 2008. Evaluating the effectiveness of best management practices using dynamic modeling. J. Environ. Eng. 134, 628–639. https://doi.org/10.1061/(ASCE)0733-9372(2008)134:8(628).

Ahern, J., Cilliers, S., Niemelä, J., 2014. The concept of ecosystem services in adaptive urban planning and design: a framework for supporting innovation. Landsc. Urban Plan. 125, 254–259. https://doi.org/10.1016/j.landurbplan.2014.01.020.

Ahiablame, L.M., Engel, B.A., Chaubey, I., 2013. Effectiveness of low impact development practices in two urbanized watersheds: retrofitting with rain barrel/cistern and porous pavement. J. Environ. Manag. 119, 151–161. https://doi.org/10.1016/j.jenvman.2013.01.019.

Alberti, M., Booth, D., Hill, K., Coburn, B., Avolio, C., Coe, S., Spirandelli, D., 2007. The impact of urban patterns on aquatic ecosystems: an empirical analysis in Puget lowland sub-basins. Landsc. Urban Plan. 80 (4), 345–361.

Arnold, C.L., Gibbons, C.J., 1996. Impervious surface coverage: the emergence of a key environmental indicator. J. Am. Plan. Assoc. 62, 243–258. https://doi.org/10.1080/01944369608975688.

Avellaneda, P.M., Jefferson, A.J., Grieser, J.M., Bush, S.A., 2017. Simulation of the cumulative hydrological response to green infrastructure. Water Resour. Res. 53, 3087–3101. https://doi.org/10.1002/2016WR019836.

Beighley, R.E., Moglen, G.E., 2002. Trend assessment in rainfall-runoff behavior in urbanizing watersheds. J. Hydrol. Eng. 7, 27–34. https://doi.org/10.1061/(ASCE)1084-0699(2002)7:1(27).

Bell, C.D., Spahr, K., Grubert, E., Stokes-Draut, J., Gallo, E., McCray, J.E., Hogue, T.S., 2019. Decision making on the gray-green stormwater infrastructure continuum. J. Sustain. Water Built Environ. 5, 04018016. https://doi.org/10.1061/JSWBAY.0000871.

Berland, A., Shiflett, S.A., Shuster, W.D., Garmestani, A.S., Goddard, H.C., Herrmann, D.L., Hopton, M.E., 2017. The role of trees in urban stormwater management. Landsc. Urban Plan. 162, 167–177. https://doi.org/10.1016/j.landurbplan.2017.02.017.

Bhaskar, A.S., Hogan, D.M., Nimmo, J.R., Perkins, K.S., 2018. Groundwater recharge amidst focused stormwater infiltration. Hydrol. Process. 32, 2058–2068. https://doi.org/10.1002/hyp.13137.

Bivand, R.S., Wong, D.W.S., 2018. Comparing implementations of global and local indicators of spatial association. TEST 27, 716–748. https://doi.org/10.1007/s11749-018-0599-x.

Blum, A.G., Ferraro, P.J., Archfield, S.A., Ryberg, K.R., 2020. Causal effect of impervious cover on annual flood magnitude for the United States. Geophys. Res. Lett. 47. https://doi.org/10.1029/2019GL086480 e2019GL086480.

Bond, N., 2015. hydrostats: hydrologic indices for daily time series data. R Package Version 02 4, 16. https://CRAN.R-project.org/package=hydrostats.

Booth, D.B., Bledsoe, B.P., 2009. Streams and urbanization. The Water Environment of Cities. Springer, Boston, MA, pp. 93–123.

Bromssen, C., Grimvall, A., 2002. Performance of partial Mann–Kendall tests for trend detection in the presence of covariates. Environmetrics: The official journal of the International Environmetrics Society 13 (1), 71–84.

Burrell, A.L., Evans, J.P., Liu, Y., 2017. Detecting dryland degradation using time series segmentation and residual trend analysis (TSS-RESTREND). Remote Sens. Environ. 197, 43–57. https://doi.org/10.1016/j.rse.2017.05.018.

Carlyle-Moses, D.E., Livesley, S., Baptista, M.D., Thom, J., Szota, C., 2020. Urban trees as green infrastructure for stormwater mitigation and use. In: Levia, D.F., Carlyle-Moses, D.E., Iida, S., Michalzik, B., Nanko, K., Tischer, A. (Eds.), Forest-Water Interactions, Ecological Studies. Springer International Publishing, Cham, pp. 397–432 https://doi.org/10.1007/978-3-030-26086-6_17.

Casey, J.A., James, P., Cushing, L., Jesdale, B.M., Morello-Frosch, R., 2017. Race, ethnicity, income concentration and 10-year change in urban greenness in the United States. Int. J. Environ. Res. Public Health 14 (12), 1546.

Chastain, R., Housman, I., Goldstein, J., Finco, M., Tenneson, K., 2019. Empirical cross sensor comparison of Sentinel-2A and 2B MSI, Landsat-8 OLI, and Landsat-7 ETM+ top of atmosphere spectral characteristics over the conterminous United States. Remote Sens. Environ. 221, 274–285.

Cherlet, M., Hutchinson, C., Reynolds, J., Hill, J., Sommer, S., von Maltitz, G., 2018. World Atlas of Desertification. Publication Office of the European Union, Luxembourg.

Chini, C.M., Canning, J.F., Schreiber, K.L., Peschel, J.M., Stillwell, A.S., 2017. The green experiment: cities, green stormwater infrastructure, and sustainability. Sustainability 9, 105. https://doi.org/10.3390/su9010105.

Clary, J., Urbonas, B., Jones, J., Strecker, E., Quigley, M., O'Brien, J., 2002. Developing, evaluating and maintaining a standardized stormwater BMP effectiveness database. Water Sci. Technol. 45, 65–73. https://doi.org/10.2166/wst.2002.0118.

Cohen, J.E., 1988. Statistical Power Analysis for the Behavioral Sciences. Lawrence Erlbaum Associates Inc, Hillsdale, NJ.

Corbane, C., Martino, P., Panagiotis, P., Aneta, F.J., Michele, M., Sergio, F., Marcello, S., Daniele, E., Gustavo, N., Thomas, K., 2020. The grey-green divide: multi-temporal analysis of greenness across 10,000 urban centres derived from the Global Human Settlement Layer (GHSL). Int. J. Digit. Earth 13, 101–118. https://doi.org/10.1080/17538947.2018.1530311.

Coville, R., Endreny, T., Nowak, D.J., 2020. Modeling the impact of urban trees on hydrology. In: Levia, D.F., Carlyle-Moses, D.E., Iida, S., Michalzik, B., Nanko, K., Tischer, A. (Eds.), Forest-Water Interactions, Ecological Studies. Springer International Publishing, Cham, pp. 459–487 https://doi.org/10.1007/978-3-030-26086-6_19.

Croissant, Y., Millo, G., 2008. Panel data econometrics in R: the plm package. J. Stat. Softw. 27. https://doi.org/10.18637/jss.v027.i02.

Czekajlo, A., Coops, N.C., Wulder, M.A., Hermosilla, T., Lu, Y., White, J.C., Van den Bosch, M., 2020. The urban greenness score: a satellite-based metric for multi-decadal characterization of urban land dynamics. Int. J. Appl. Earth Obs. Geoinf. 93, 102210.

Daly, C., Halbleib, M., Smith, J.I., Gibson, W.P., Doggett, M.K., Taylor, G.H., Curtis, J., Pasteris, P.P., 2008. Physiographically sensitive mapping of climatological temperature and precipitation across the conterminous United States. Int. J. Climatol. 28, 2031–2064. https://doi.org/10.1002/joc.1688.

Davis, A.P., 2007. Field performance of bioretention: water quality. Environ. Eng. Sci. 24, 1048–1064. https://doi.org/10.1089/ees.2006.0190.

De Cicco, L.A., Lorenz, D., Hirsch, R.M., Watkins, W., 2018. dataRetrieval: R Packages for Discovering and Retrieving Water Data Available From US Federal Hydrologic Web Services. US Geol. Surv, Rest. VA https://doi.org/10.5066/P9X4L3GE.

Dietz, M.E., Clausen, J.C., 2008. Stormwater runoff and export changes with development in a traditional and low impact subdivision. J. Environ. ManageMicrobial and Nutrient Contaminants of Fresh and Coastal Waters 87, 560–566. https://doi.org/10.1016/j.jenvman.2007.03.026.

Dussaillant, A.R., Cuevas, A., Potter, K.W., 2005. Raingardens for stormwater infiltration and focused groundwater recharge: simulations for different world climates. Water Supply 5, 173–179. https://doi.org/10.2166/ws.2005.0097.

Ebrahimian, A., Gulliver, J.S., Wilson, B.N., 2018. Estimating effective impervious area in urban watersheds using land cover, soil character and asymptotic curve number. Hydrol. Sci. J. 63 (4), 513–526.

Ebrahimian, A., Wadzuk, B., Traver, R., 2019. Evapotranspiration in green stormwater infrastructure systems. Sci. Total Environ. 688, 797–810.

Fahy, B., Chang, H., 2019. Effects of stormwater green infrastructure on watershed outflow: does spatial distribution matter? Int. J. Geospat. Environ. Res. 6.

Falcone, J.A., Carlisle, D.M., Wolock, D.M., Meador, M.R., 2010. GAGES: a stream gage database for evaluating natural and altered flow conditions in the conterminous United States. Ecology 91, 621. https://doi.org/10.1890/09-0889.1.

Faul, F., Erdfelder, E., Lang, A.-G., Buchner, A., 2007. G*Power 3: a flexible statistical power analysis program for the social, behavioral, and biomedical sciences. Behav. Res. Methods 39 (2), 175–191. https://doi.org/10.3758/BF03193146.

Fitzgerald, J., Laufer, J., 2017. Governing green stormwater infrastructure: the Philadelphia experience. Local Environ. 22, 256–268. https://doi.org/10.1080/13549839.2016.1191063.

Gan, M., Deng, J., Zheng, X., Hong, Y., Wang, K., 2014. Monitoring urban greenness dynamics using multiple endmember spectral mixture analysis. PLOS ONE 9, e112202. https://doi.org/10.1371/journal.pone.0112202.

Golden, H.E., Hoghooghi, N., 2018. Green infrastructure and its catchment-scale effects: an emerging science. WIREs Water 5, e1254. https://doi.org/10.1002/wat2.1254.

Gong, P., Li, X., Wang, J., Bai, Y., Chen, B., Hu, T., Liu, X., Xu, B., Yang, J., Zhang, W., Zhou, Y., 2020. Annual maps of global artificial impervious area (GAIA) between 1985 and 2018. Remote Sens. Environ. 236, 111510. https://doi.org/10.1016/j.rse.2019.111510.

Gorelick, N., Hancher, M., Dixon, M., Ilyushchenko, S., Thau, D., Moore, R., 2017. Google Earth Engine: planetary-scale geospatial analysis for everyone. Remote Sens. EnvironBig Remotely Sensed Data: tools, applications and experiences 202, 18–27. https://doi.org/10.1016/j.rse.2017.06.031.

Gunder, M., Hillier, J., 2016. Planning in Ten Words or Less: A Lacanian Entanglement with Spatial Planning. Routledge, London https://doi.org/10.4324/9781315246697.

Hager, G.W., Belt, K.T., Stack, W., Burgess, K., Grove, J.M., Caplan, B., Hardcastle, M., Shelley, D., Pickett, S.T., Groffman, P.M., 2013. Socioecological revitalization of an urban watershed. Front. Ecol. Environ. 11, 28–36. https://doi.org/10.1890/120069.

Hale, R.L., 2016. Spatial and temporal variation in local stormwater infrastructure use and stormwater management paradigms over the 20th century. Water 8, 310. https://doi.org/10.3390/w8070310.

Hausman, J.A., 1978. Specification tests in econometrics. Econometrica 46, 1251–1271. https://doi.org/10.2307/1913827.

Hoghooghi, N., Golden, H.E., Bledsoe, B.P., Barnhart, B.L., Brookes, A.F., Djang, K.S., Halama, J.J., McKane, R.B., Nietch, C.T., Pettus, P.P., 2018. Cumulative effects of low impact development on watershed hydrology in a mixed land-cover system. Water 10, 991. https://doi.org/10.3390/w10080991.

Holman-Dodds, J.K., Bradley, A.A., Potter, K.W., 2003. Evaluation of hydrologic benefits of infiltration based urban storm water management1. J. Am. Water Resour. Assoc. 39, 205–215. https://doi.org/10.1111/j.1752-1688.2003.tb01572.x.

Homer, C., Dewitz, J., Jin, S., Xian, G., Costello, C., Danielson, P., Gass, L., Funk, M., Wickham, J., Stehman, S., Auch, R., Riitters, K., 2020. Conterminous United States land cover change patterns 2001–2016 from the 2016 National Land Cover Database. ISPRS J. Photogramm. Remote Sens. 162, 184–199. https://doi.org/10.1016/j.isprsjprs.2020.02.019.

Jarden, K.M., Jefferson, A.J., Grieser, J.M., 2016. Assessing the effects of catchment-scale urban green infrastructure retrofits on hydrograph characteristics. Hydrol. Process. 30, 1536–1550. https://doi.org/10.1002/hyp.10736.

Kanniah, K.D., Muhamad, N., Kang, C.S., 2014. Remote sensing assessment of carbon storage by urban forest. IOP Conf. Ser. Earth Environ. Sci. 18, 012151. https://doi.org/10.1088/1755-1315/18/1/012151.

Kong, F., Ban, Y., Yin, H., James, P., Dronova, I., 2017. Modeling stormwater management at the city district level in response to changes in land use and low impact development. Environ. Model. Softw. 95, 132–142. https://doi.org/10.1016/j.envsoft.2017.06.021.

Li, H., 2015. Green infrastructure for highway stormwater management: field investigation for future design, maintenance, and management needs. J. Infrastruct. Syst. 21, 05015001. https://doi.org/10.1061/(ASCE)IS.1943-555X.0000248.

Libiseller, C., Grimvall, A., 2002. Performance of partial mann-kendall tests for trend detection in the presence of covariates. Environmetrics 13, 71–84. https://doi.org/10.1002/env.507.

Loftis, J.C., MacDonald, L.H., Streett, S., Iyer, H.K., Bunte, K., 2001. Detecting cumulative watershed effects: the statistical power of pairing. J. Hydrol. 251, 49–64. https://doi.org/10.1016/S0022-1694(01)00431-0.

Loperfido, J.V., Noe, G.B., Jarnagin, S.T., Hogan, D.M., 2014. Effects of distributed and centralized stormwater best management practices and land cover on urban stream hydrology at the catchment scale. J. Hydrol. Water Gov. Across Competing Scales Coupling Land Water Management 519, 2584–2595. https://doi.org/10.1016/j.jhydrol.2014.07.007.

Lyne, V., Hollick, M., 1979. Stochastic time-variable rainfall-runoff modelling. Institute of Engineers Australia National Conference. Institute of Engineers Australia Barton, Australia, pp. 89–93.

Maestre, A., Pitt, R., 2005. The National Stormwater Quality Database, Version 1.1, a Compilation and Analysis of NPDES Stormwater Monitoring Information. US EPA Off, Water Wash. DC.

Mancino, G., Ferrara, A., Padula, A., Nole, A., 2020. Cross-comparison between Landsat 8 (OLI) and Landsat 7 (ETM+) derived vegetation indices in a Mediterranean environment. Remote Sens. 12 (2), 291.

McDonald, R.I., 2015. Conservation for Cities: How to Plan & Build Natural Infrastructure. Island Press, Washington, D.C.

McDonald, R.I., Biswas, T., Sachar, C., Housman, I., Boucher, T.M., Balk, D., Nowak, D., Spotswood, E., Stanley, C.K., Leyk, S., 2021. The tree cover and temperature disparity in US urbanized areas: quantifying the association with income across 5,723 communities. PLOS ONE 16, e0249715. https://doi.org/10.1371/journal.pone.0249715.

McPhillips, L.E., Matsler, A.M., 2018. Temporal evolution of green stormwater infrastructure strategies in three US cities. Front. Built Environ. 4, 26. https://doi.org/10.3389/fbuil.2018.00026.

Melchiorri, M., Florczyk, A.J., Freire, S., Schiavina, M., Pesaresi, M., Kemper, T., 2018. Unveiling 25 years of planetary urbanization with remote sensing: perspectives from the global human settlement layer. Remote Sens. 10, 768. https://doi.org/10.3390/rs10050768.

Miura, T., Huete, A.R., Yoshioka, H., 2000. Evaluation of sensor calibration uncertainties on vegetation indices for MODIS. IEEE Trans. Geosci. Remote Sens. 38, 1399–1409.

Mu, Q., Zhao, M., Running, S.W., 2011. Improvements to a MODIS global terrestrial evapotranspiration algorithm. Remote Sens. Environ. 115, 1781–1800. https://doi.org/10.1016/j.rse.2011.02.019.

Mu, Q., Zhao, M., Running, S.W., 2013. MODIS global terrestrial evapotranspiration (ET) product (NASA MOD16A2/A3). Algorithm Theor. Basis Doc. Collect. 5, p. 600.

Myneni, R.B., Hall, F.G., Sellers, P.J., Marshak, A.L., 1995. The interpretation of spectral vegetation indexes. IEEE Trans. Geosci. Remote Sens. 33 (2), 481–486.

Nieto, S., Flombaum, P., Garbulsky, M.F., 2015. Can temporal and spatial NDVI predict regional bird-species richness? Glob. Ecol. Conserv. 3, 729–735. https://doi.org/10.1016/j.gecco.2015.03.005.

Nowak, D.J., Greenfield, E.J., 2010. Evaluating the National Land Cover Database tree canopy and impervious cover estimates across the conterminous United States: a comparison with photo-interpreted estimates. Environ. Manag. 46, 378–390. https://doi.org/10.1007/s00267-010-9536-9.

Nowak, D.J., Greenfield, E.J., 2020. The increase of impervious cover and decrease of tree cover within urban areas globally (2012–2017). Urban For. Urban Green. 49, 126638.

O'Driscoll, C., Lachapelle, G., Tamazin, M.E., 2010. Investigation of the benefits of combined GPS/GLONASS receivers in urban environments. Proceeding on RIN NAV10 Conference on Position, Location, Timing: Everyone, Everything, Everywhere.

Pennino, M.J., McDonald, R.I., Jaffe, P.R., 2016. Watershed-scale impacts of stormwater green infrastructure on hydrology, nutrient fluxes, and combined sewer overflows in the mid-Atlantic region. Sci. Total Environ. 565, 1044–1053. https://doi.org/10.1016/j.scitotenv.2016.05.101.

Perez-Pedini, C., Limbrunner, J.F., Vogel, R.M., 2005. Optimal location of infiltration-based best management practices for storm water management. J. Water Resour. Plan. Manag. 131 (6), 441–448.

Pesaresi, M., Ehrlich, D., Ferri, S., Florczyk, A., Freire, S., Halkia, M., Julea, A., Kemper, T., Soille, P., Syrris, V., 2016. Operating procedure for the production of the Global Human Settlement Layer from Landsat data of the epochs 1975, 1990, 2000, and 2014. Publ. Off. Eur. Union 1–62.

Pohlert, T., Pohlert, M.T., Kendall, S., 2016. R Package 'trend.' Non-Parametr. Trend Tests Change-Point Detect.

Price, K., 2011. Effects of watershed topography, soils, land use, and climate on baseflow hydrology in humid regions: a review. Prog. Phys. Geogr. Earth Environ. 35, 465–492. https://doi.org/10.1177/0309133311402714.

Prudencio, L., Null, S.E., 2018. Stormwater management and ecosystem services: a review. Environ. Res. Lett. 13, 033002. https://doi.org/10.1088/1748-9326/aaa81a.

R Core Team, 2018. R: A Language and Environment for Statistical Computing. Austria, Vienna.

Rani, M., Kumar, P., Pandey, P.C., Srivastava, P.K., Chaudhary, B.S., Tomar, V., Mandal, V.P., 2018. Multi-temporal NDVI and surface temperature analysis for Urban Heat Island inbuilt surrounding of sub-humid region: a case study of two geographical regions. Remote Sens. Appl. Soc. Environ. 10, 163–172. https://doi.org/10.1016/j.rsase.2018.03.007.

Roy, A.H., Wenger, S.J., Fletcher, T.D., Walsh, C.J., Ladson, A.R., Shuster, W.D., Thurston, H.W., Brown, R.R., 2008. Impediments and solutions to sustainable, watershed-scale urban stormwater management: lessons from Australia and the United States. Environ. Manag. 42, 344–359. https://doi.org/10.1007/s00267-008-9119-1.

Roy, A.H., Rhea, L.K., Mayer, A.L., Shuster, W.D., Beaulieu, J.J., Hopton, M.E., Morrison, M.A., Amand, A.S., 2014. How much is enough? Minimal responses of water quality and stream biota to partial retrofit stormwater management in a suburban neighborhood. PLOS ONE 9, e85011. https://doi.org/10.1371/journal.pone.0085011.

Roy, D.P., Kovalskyy, V., Zhang, H.K., Vermote, E.F., Yan, L., Kumar, S.S., Egorov, A., 2016. Characterization of Landsat-7 to Landsat-8 reflective wavelength and normalized difference vegetation index continuity. Remote Sens. Environ. Landsat 8 Sci.Results 185, 57–70. https://doi.org/10.1016/j.rse.2015.12.024.

Rugel, E.J., Henderson, S.B., Carpiano, R.M., Brauer, M., 2017. Beyond the Normalized Difference Vegetation Index (NDVI): developing a Natural Space Index for population-level health research. Environ. Res. 159, 474–483. https://doi.org/10.1016/j.envres.2017.08.033.

Sarkar, S., Butcher, J.B., Johnson, T.E., Clark, C.M., 2018. Simulated sensitivity of urban green infrastructure practices to climate change. Earth Interact. 22, 1–37. https://doi.org/10.1175/EI-D-17-0015.1.

Selbig, W.R., Loheide II, S.P., Shuster II, W., Scharenbroch II, B.C., Coville II, R.C., Kruegler II, J., Avery II, W., Haefner II, R., Nowak II, D., 2021. Quantifying the stormwater runoff volume reduction benefits of urban street tree canopy. Sci. Total Environ. 151296.

Sen, P.K., 1968. Estimates of the regression coefficient based on Kendall's tau. J. Am. Stat. Assoc. 63, 1379–1389. https://doi.org/10.1080/01621459.1968.10480934.

Shuster, W.D., Bonta, J., Thurston, H., Warnemuende, E., Smith, D.R., 2005. Impacts of impervious surface on watershed hydrology: a review. Urban Water J. 2 (4), 263–275.

Smith, E.P., Rose, K.A., 1991. Trend detection in the presence of covariates: stagewise versus multiple regression. Environmetrics 2, 153–168. https://doi.org/10.1002/env.3770020204.

Spahr, K.M., Bell, C.D., McCray, J.E., Hogue, T.S., 2020. Greening up stormwater infrastructure: measuring vegetation to establish context and promote cobenefits in a diverse set of US cities. Urban For. Urban Green. 48, 126548. https://doi.org/10.1016/j.ufug.2019.126548.

Spahr, K.M., Bell, C.D., Gallo, E.M., McCray, J.E., Hogue, T.S., 2021. Incorporating a multiple-benefit analysis into a stormwater decision-support tool at planning level. J. Sustain. Water Built Environ. 7, 04021011. https://doi.org/10.1061/JSWBAY.0000952.

Steinschneider, S., Yang, Y.-C.E., Brown, C., 2013. Panel regression techniques for identifying impacts of anthropogenic landscape change on hydrologic response. Water Resour. Res. 49, 7874–7886. https://doi.org/10.1002/2013WR013818.

Strecker, E.W., Quigley, M.M., Urbonas, B., Jones, J., 2004. Analyses of the expanded EPA/ASCE international BMP database and potential implications for BMP design. Proceedings of the World Water and Environmental Resources Congress 2004. Salt Lake City, Utah, pp. 1–10.

Tan, Xuejin, Liu, B., Tan, Xuezhi, 2020. Global changes in baseflow under the impacts of changing climate and vegetation. Water Resour. Res. 56. https://doi.org/10.1029/2020WR027349 e2020WR027349.

Tao, J., Li, Z., Peng, X., Ying, G., 2017. Quantitative analysis of impact of green stormwater infrastructures on combined sewer overflow control and urban flooding control. Front. Environ. Sci. Eng. 11, 11. https://doi.org/10.1007/s11783-017-0952-4.

Venkataramanan, V., Lopez, D., McCuskey, D.J., Kiefus, D., McDonald, R.I., Miller, W.M., Packman, A.I., Young, S.L., 2020. Knowledge, attitudes, intentions, and behavior related to green infrastructure for flood management: a systematic literature review. Sci. Total Environ. 720, 137606. https://doi.org/10.1016/j.scitotenv.2020.137606.

Venter, Z.S., Shackleton, C.M., Van Staden, F., Selomane, O., Masterson, V.A., 2020. Green Apartheid: urban green infrastructure remains unequally distributed across income and race geographies in South Africa. Landsc. Urban Plan. 203, 103889.

Vogel, J.R., Moore, T.L., Coffman, R.R., Rodie, S.N., Hutchinson, S.L., McDonough, K.R., McLemore, A.J., McMaine, J.T., 2015. Critical review of technical questions facing low impact development and green infrastructure: a perspective from the Great Plains. Water Environ. Res. 87, 849–862. https://doi.org/10.2175/106143015X14362865226392.

Walsh, C.J., Roy, A.H., Feminella, J.W., Cottingham, P.D., Groffman, P.M., Morgan, R.P., 2005. The urban stream syndrome: current knowledge and the search for a cure. J. North Am. Benthol. Soc. 24, 706–723. https://doi.org/10.1899/04-028.1.

Wang, R., Eckelman, M.J., Zimmerman, J.B., 2013. Consequential environmental and economic life cycle assessment of green and gray stormwater infrastructures for combined sewer systems. Environ. Sci. Technol. 47, 11189–11198. https://doi.org/10.1021/es4026547.

Wolf, K.L., Lam, S.T., McKeen, J.K., Richardson, G.R.A., van den Bosch, M., Bardekjian, A.C., 2020. Urban trees and human health: a scoping review. Int. J. Environ. Res. Public Health 17, 4371. https://doi.org/10.3390/ijerph17124371.

Yang, B., Li, S., 2013. Green infrastructure design for stormwater runoff and water quality: empirical evidence from large watershed-scale community developments. Water 5, 2038–2057. https://doi.org/10.3390/w5042038.

Zellner, M., Massey, D., Minor, E., Gonzalez-Meler, M., 2016. Exploring the effects of green infrastructure placement on neighborhood-level flooding via spatially explicit simulations. Comput. Environ. Urban. Syst. 59, 116–128. https://doi.org/10.1016/j.compenvurbsys.2016.04.008.

Zhu, Z., Woodcock, C.E., Holden, C., Yang, Z., 2015. Generating synthetic Landsat images based on all available Landsat data: predicting Landsat surface reflectance at any given time. Remote Sens. Environ. 162, 67–83. https://doi.org/10.1016/j.rse.2015.02.009.

Zhu, Z., Piao, S., Myneni, R.B., Huang, M., Zeng, Z., Canadell, J.G., Ciais, P., Sitch, S., Friedlingstein, P., Arneth, A., Cao, C., Cheng, L., Kato, E., Koven, C., Li, Y., Lian, X., Liu, Y., Liu, R., Mao, J., Pan, Y., Peng, S., Peñuelas, J., Poulter, B., Pugh, T.A.M., Stocker, B.D., Viovy, N., Wang, X., Wang, Y., Xiao, Z., Yang, H., Zaehle, S., Zeng, N., 2016. Greening of the Earth and its drivers. Nat. Clim. Chang. 6, 791–795. https://doi.org/10.1038/nclimate3004.

USGS, 2020. Landsat was accessed on 6/6/2020 from https://registry.opendata.aws/usgs-landsat.